Expanded View Figures

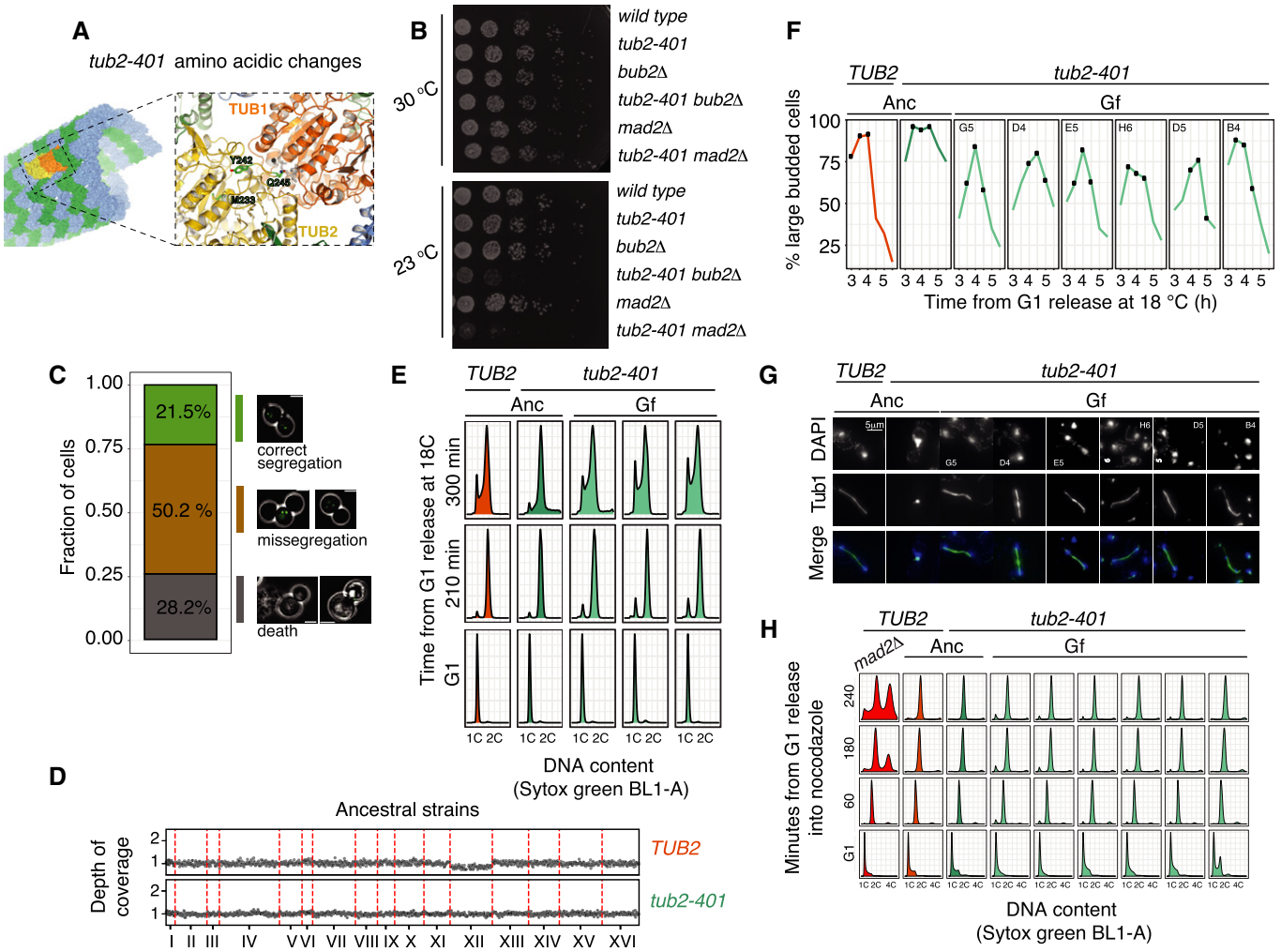

Figure EV1. Characterization of evolved cells.

A The three amino acid changes of the *tub2-401* allele.

B Serial 5-fold dilution of cells of the indicated genotypes spotted on YPD and incubated at the indicated temperatures.

C Different fates of *tub2-401* cells growing at 18°C (correct chromosome segregation after rebudding, missegregation after rebudding, or death before rebudding). Cells were synchronized in G1, released at 18°C to express the *tub2-401* phenotype, and imaged every hour for 41 h in a microfluidic chamber. The events of segregation were identified by following GFP-tagged chromosome V. Among the 21.5% of cells correctly segregating, 44.4% died before the end of the movie and 55.5% did not. Among the 50.2% of cell missegregating, 48.5% died before the end of the movie and 51.4% did not. Cells that neither died nor rebudded by the end of the movie (12 out of 221 cells from 2 biological replicates) are not included in this analysis. Scale bars are 5 μm long. Every image, except the leftmost "death", have the same contrast settings. See Movie EV1.

D Normalized and corrected depth of coverage for the two ancestral strains. Each dot represents the median depth over a 10,000 bp window.

E Ancestral cells and selected Gf populations (G5, D5 and H6) were synchronized in G1 at 30°C and released at 18°C, as explained in Materials and Methods. Cells were collected 3.5 and 5 h after G1 release. DNA content was assessed by Sytox Green staining.

F Selected Gf populations (G5, D4, E5, H6, D5, and B4) and ancestors were synchronized in G1 at 30°C and released at 18°C, as explained in Materials and Methods. The fraction of cells with a large bud was monitored every 30 min from 3 to 5 h after G1 release. Black dots identify the timepoints in which spindle lengths were measured. The kinetics is representative of one biological replicate.

G Representative spindles in Ancestor and selected Gf cells. Tub1 was stained for immunofluorescence, while nuclei were stained with DAPI. Images are examples from one biological replicate.

H *mad2Δ*, ancestral cells, and selected Gf populations (the same as in Fig 1D and E) were synchronized in G1 at 30°C and released in nocodazole 15 μg/ml. Cells were collected 1, 3, and 4 h after nocodazole addition. DNA content was assessed by Sytox Green staining.

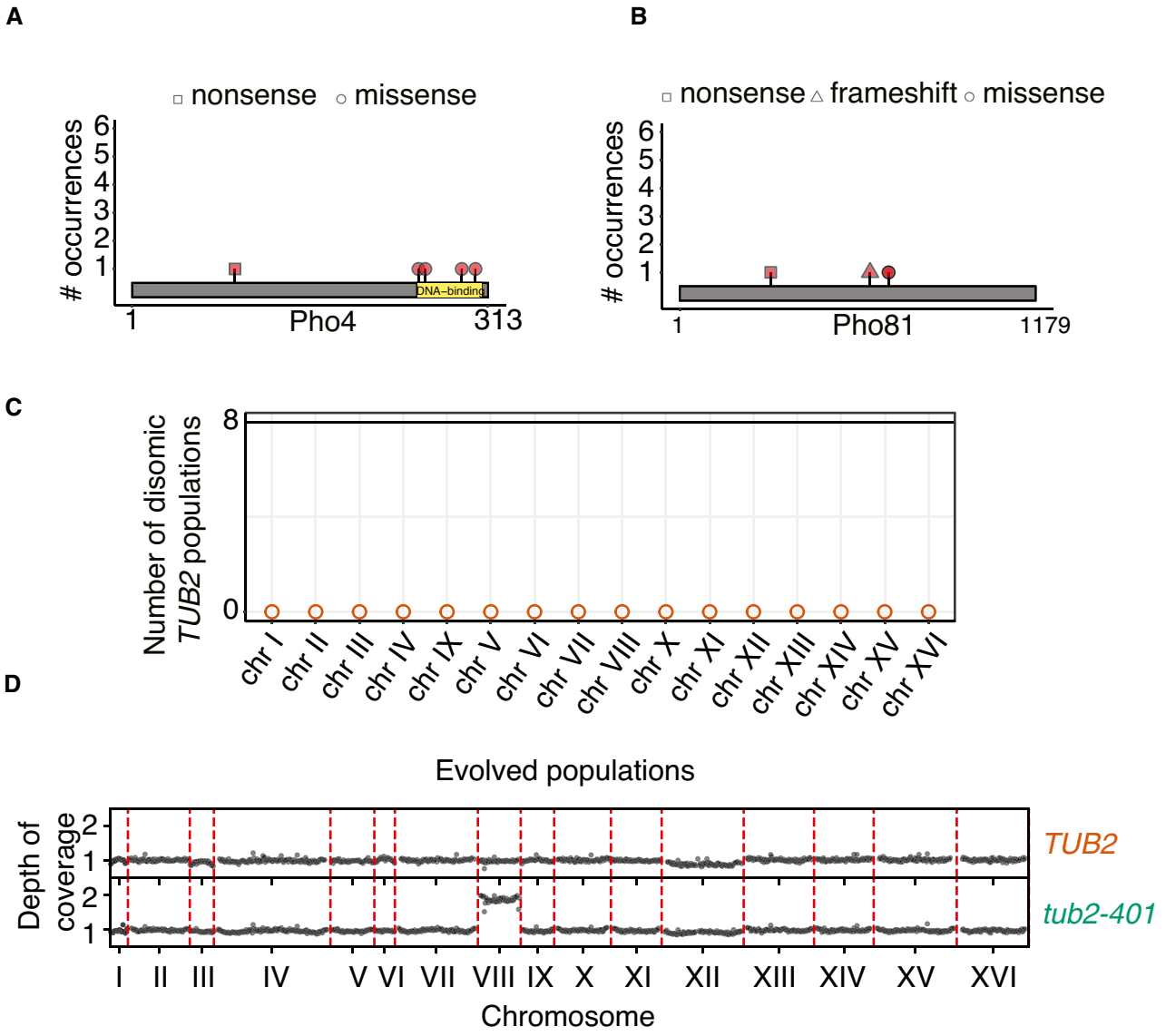

Figure EV2. Recurrent amino acid changes and disomies in evolved *TUB2*.

A, B Amino acid changes caused by mutations occurring independently multiple times in *PHO81* and *PHO4*. They were detected only in *TUB2* cells (Fig 3A)

C Lack of disomic populations among the eight evolving *TUB2* populations. Empty dots are used to mark chromosomes that are monosomic in every population. Chromosome copy numbers were determined by coverage analysis (an example in Fig EV2D).

D Normalized and corrected depth of coverage for two representative samples (*TUB2*, population A1; *tub2-401*, population A4). Each dot represents the median depth over a 10,000 bp window.

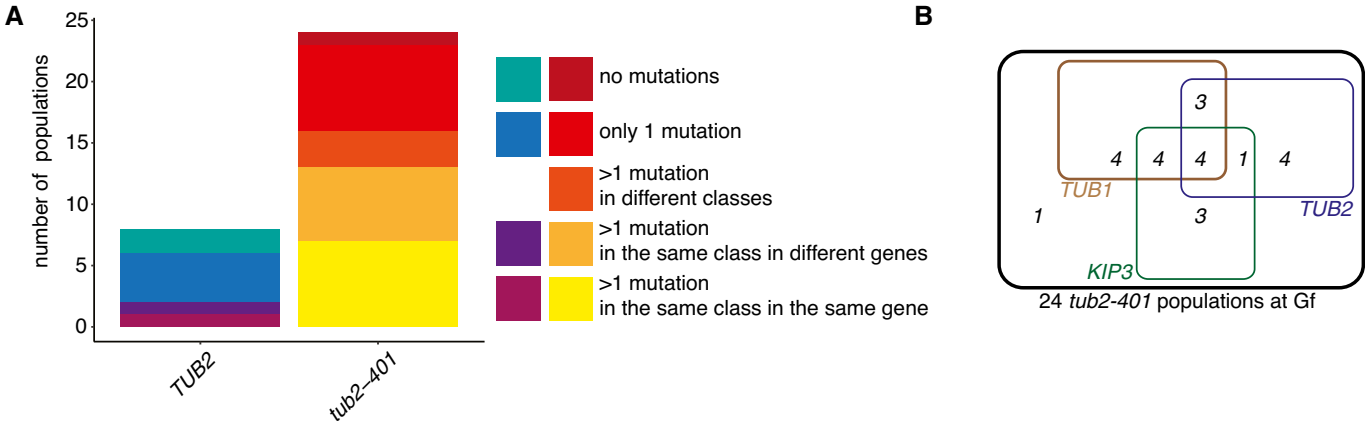

Figure EV3. Mutation frequencies at final timepoint (Gf) in *TUB2* and *tub2-401* evolved populations.

A Bar plot of populations grouped according to the presence of multiple mutations in recurrently mutated genes, detected by NGS at the end of the experiment (Gf).

B Venn Diagram of *tub2-401* populations at Gf, carrying mutations in *TUB2*, *TUB1* or *KIP3* (data shown in the third panel from top of Fig 3A).

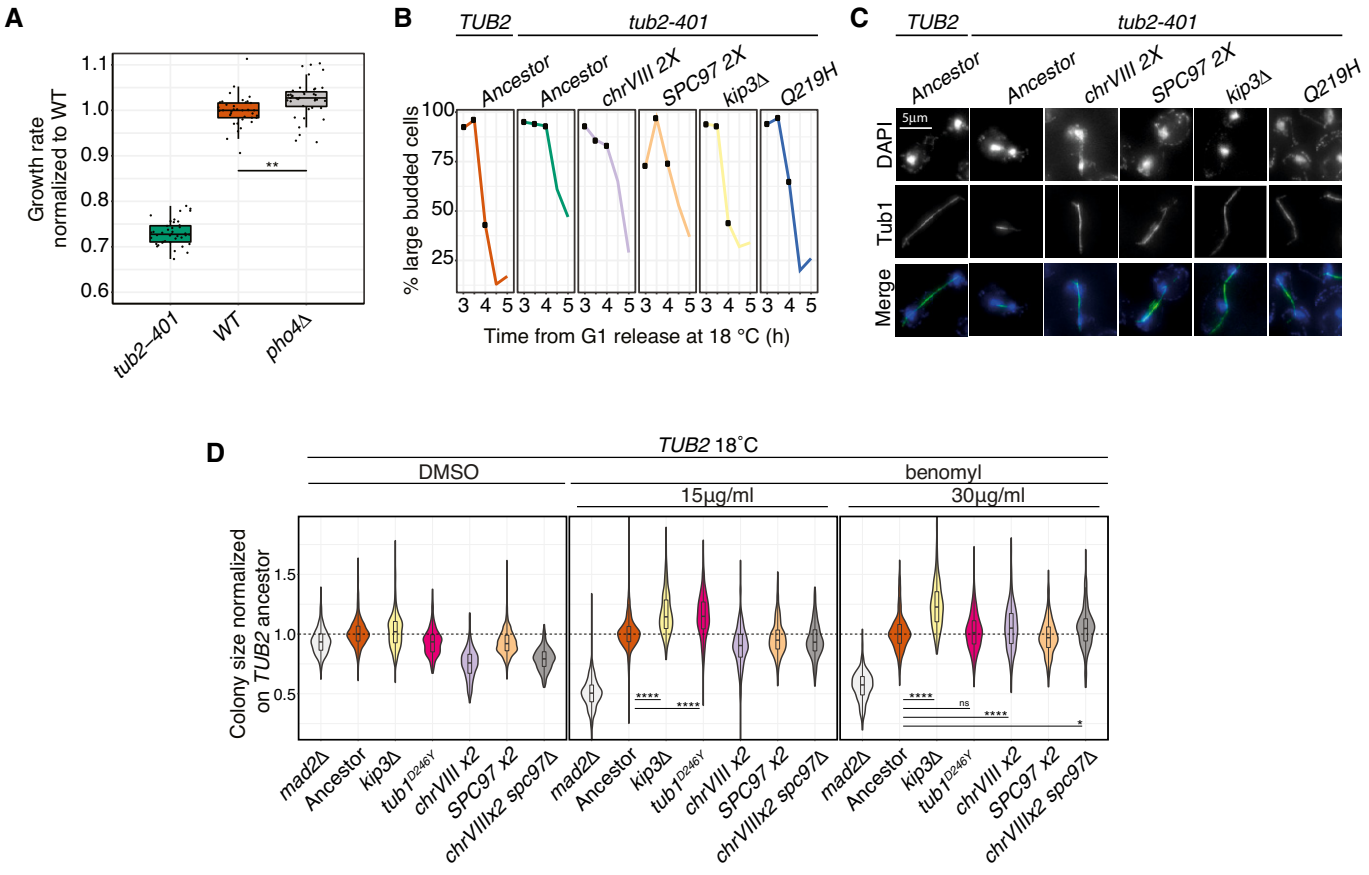

Figure EV4.

Figure EV4. Characterization of engineered strains.

A Growth rates of *wt*, *tub2-401* and *pho4Δ* cells were measured with *in liquid* growth assays. Experiments were performed at 18°C after growing cells at 18°C for 24 h. Growth rates result from fitting optical density over time with an exponential (see Materials and Methods for details). Pairwise strain comparisons were made using a linear model, adjusting for batch effects for experiments performed on different days. Symbols refer to the *P*-values of the strain comparison (**P-value $< 10^{-2}$). The plot includes three biological replicates, each with ~12 technical replicates per strain. The boxes span the interquartile range (IQR, from the 25th to the 75th percentiles), and the central band represents the median. The lower (upper) whisker extends from the box to the smallest (largest) value no further than 1.5*IQR from the box. Individual measures are plotted as dots.

B–C Spindles measurements in *tub2-401* cells carrying adaptive mutations. Cells were synchronized in G1 at 30°C and released at 18°C as explained in Materials and Methods. (B) The fraction of large-budded cells (dumbell) was monitored every 30 min from 3 to 5 h after G1 release. Black dots identify the timepoints in which the spindle lengths were measured (Fig 5E). The kinetics is representative of one biological replicate (C) Representative spindles. Microtubules were identified by immunofluorescence on Tub1 while nuclei were stained with DAPI. Images are examples from one biological replicate.

D Measurement of colony size on agar plates as a proxy for growth. Colonies of the specified genotypes grew on YPD agar plates at 30°C before being pinned onto YPD agar plates supplemented with 1% DMSO with or without the spindle poison benomyl (15 μg/ml or 30 μg/ml final concentrations). The plot includes seven biological replicates for every strain but *chrVIII spc97Δ*, which is present in 3. The number of colonies included in the DMSO panel are, from left to right: 753 *mad2Δ*, 750 ancestor *TUB2*, 750 *kip3Δ*, 753 *tub1^{D246Y}*, 753 *chrVIII 2X*, 756 *SPC97 2X*, 321 *chrVIII 2X spc97Δ*. The number of colonies included in the benomyl 15μg/ml panel are, from left to right: 611 *mad2Δ*, 649 ancestor *TUB2*, 613 *kip3Δ*, 673 *tub1^{D246Y}*, 684 *chrVIII 2X*, 650 *SPC97 2X*, 291 *chrVIII 2X spc97Δ*. The number of colonies included in the benomyl 30μg/ml panel are, from left to right: 642 *mad2Δ*, 669 ancestor *TUB2*, 627 *kip3Δ*, 694 *tub1^{D246Y}*, 665 *chrVIII 2X*, 645 *SPC97 2X*, 303 *chrVIII 2X spc97Δ*. Pairwise strain comparisons were made using a linear model, adjusting for batch effects for experiments performed on different days. For each statistical comparison, the linear model coefficients and the resulting *P*-values are, from left to right: 0.167 (P ~10^{-70}), 0.143 (P ~10^{-55}), 0.231 (P ~10^{-105}), 0.007 (P ~10^{-1}), 0.037 (P ~10^{-5}), 0.032 (P ~10^{-2}). Plates were incubated at 18°C and imaged after 2 days. Colony size is normalized on the *TUB2* ancestor. In every panel, violin plots show the densities along the *y*-axis smoothed with a Gaussian kernel, while the boxes span the interquartile range (IQR, from the 25th to the 75th percentiles). The central band represents the median. The lower (upper) whisker extends from the box to the smallest (largest) value no further than 1.5*IQR from the box. See Materials and Methods for details.

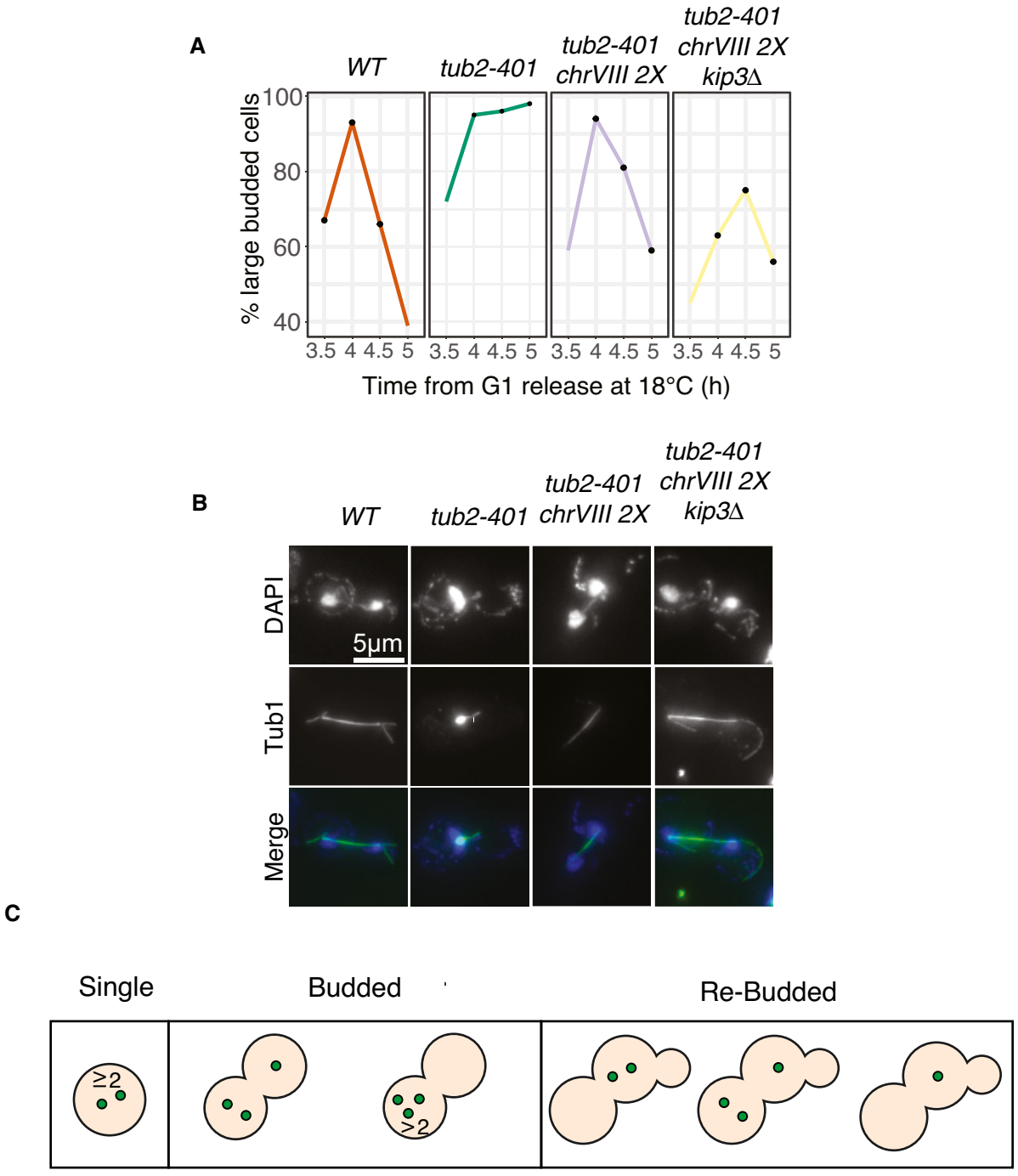

Figure EV5. Characterization of microtubule function in Gr and Gf.

A Cells were synchronized in G1 at 30°C and released at 18°C, as explained in Materials and Methods. The fraction of cells with a large bud was monitored every 30 min from 3.5 to 5 h after G1 release. Black dots identify the timepoints in which the spindle lengths were measured (see Fig 7B). The kinetics is representative of one the biological replicate.

B Representative spindles of the different strains shown in Fig 7B. Tub1 was stained for immunofluorescence, while nuclei were stained with DAPI. Images are examples from one biological replicate.

C Morphologies of cells that were scored as missegregated in Fig 7C based on the number of chrV-GFP dots. Budded cells with two dots in the mother cell could not be attributed as missegregated, since they could either end up segregating properly or missegregating, as observed in Movie EV1. In the movie, the proper assignment was based on the pattern of budding (e.g., cells that kept two dots after budding were assigned as missegregated), similarly to what done here.

Figure EV6. Overlap of residues mutated in human patients and evolved yeast.

Taking advantage of a database which includes mutations found in beta-tubulin across eukaryotes (https://tubulinmutations.bio.uci.edu/), we identified beta-tubulin residues mutated in cancer patients (37). The total number of entries in the database gave us an estimate of the upper limit for the number of residues that can be mutated in yeast and mammals (289). During the evolution experiment, we observed mutations in eight different residues. Of these mutations 4 are among the 37 found in cancer patients, which is a statistically significant overlap (*P*-value 0.011, hypergeometric test). Notice that even though not all residues are conserved, superposition of mammalian beta-tubulin with Tub2 (carried out on 419 C-alpha's, with a RMSD of 1.01 Å) reveals that all the residues emerging in our study spatially overlap with the corresponding counterparts of mammalian beta-tubulin highlighted in the sequence alignment. However, the result remains statistically significant including only residues conserved between yeast and at least one human isoform.

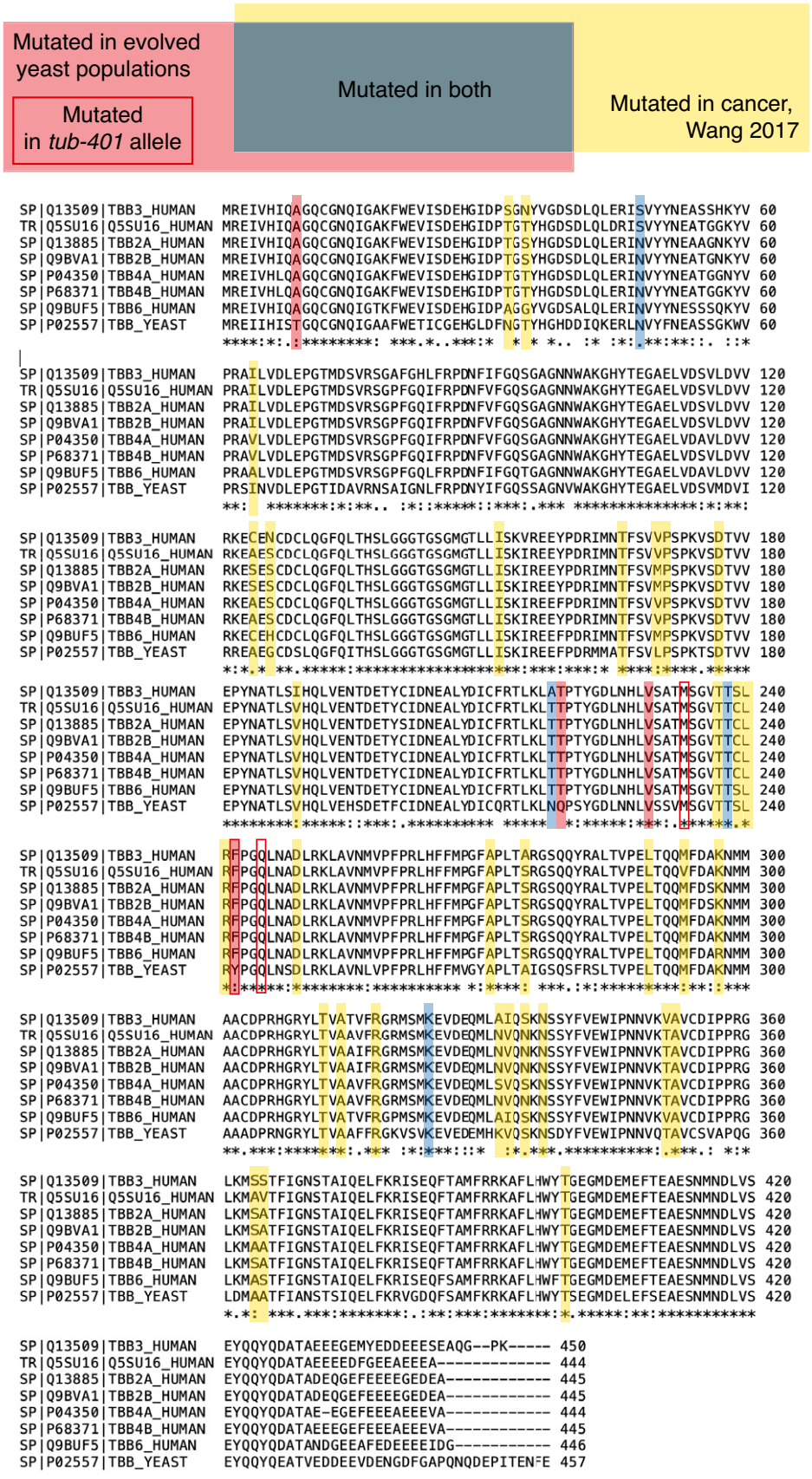

Figure EV6.